

Aberystwyth University

Atomic and vibrational origins of mechanical toughness in bioactive cement during setting

Tian, Kun V.; Yang, Bin; Yue, Yuanzheng; Bowron, Daniel T.; Mayers, Jerry; Donnan, Robert S.; Dobó-nagy, Csaba; Nicholson, John W.; Fang, De-cai; Greer, A. Lindsay; Chass, Gregory A.; Greaves, G. Neville

Published in:

Nature Communications

DOI:

[10.1038/ncomms9631](https://doi.org/10.1038/ncomms9631)

Publication date:

2015

Citation for published version (APA):

Tian, K. V., Yang, B., Yue, Y., Bowron, D. T., Mayers, J., Donnan, R. S., Dobó-nagy, C., Nicholson, J. W., Fang, D., Greer, A. L., Chass, G. A., & Greaves, G. N. (2015). Atomic and vibrational origins of mechanical toughness in bioactive cement during setting. *Nature Communications*, 6, Article 8631. <https://doi.org/10.1038/ncomms9631>

Document License

CC BY

General rights

Copyright and moral rights for the publications made accessible in the Aberystwyth Research Portal (the Institutional Repository) are retained by the authors and/or other copyright owners and it is a condition of accessing publications that users recognise and abide by the legal requirements associated with these rights.

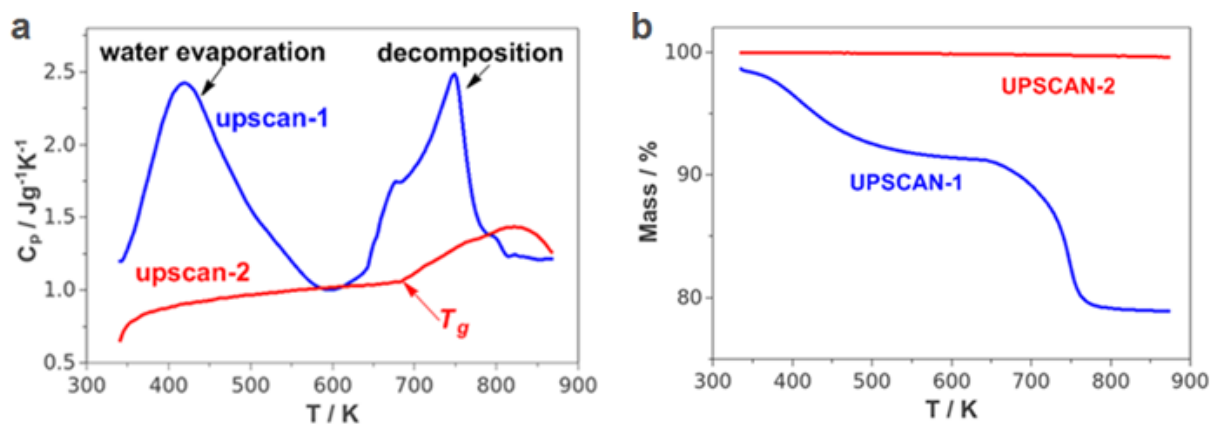
- Users may download and print one copy of any publication from the Aberystwyth Research Portal for the purpose of private study or research.
- You may not further distribute the material or use it for any profit-making activity or commercial gain
- You may freely distribute the URL identifying the publication in the Aberystwyth Research Portal

Take down policy

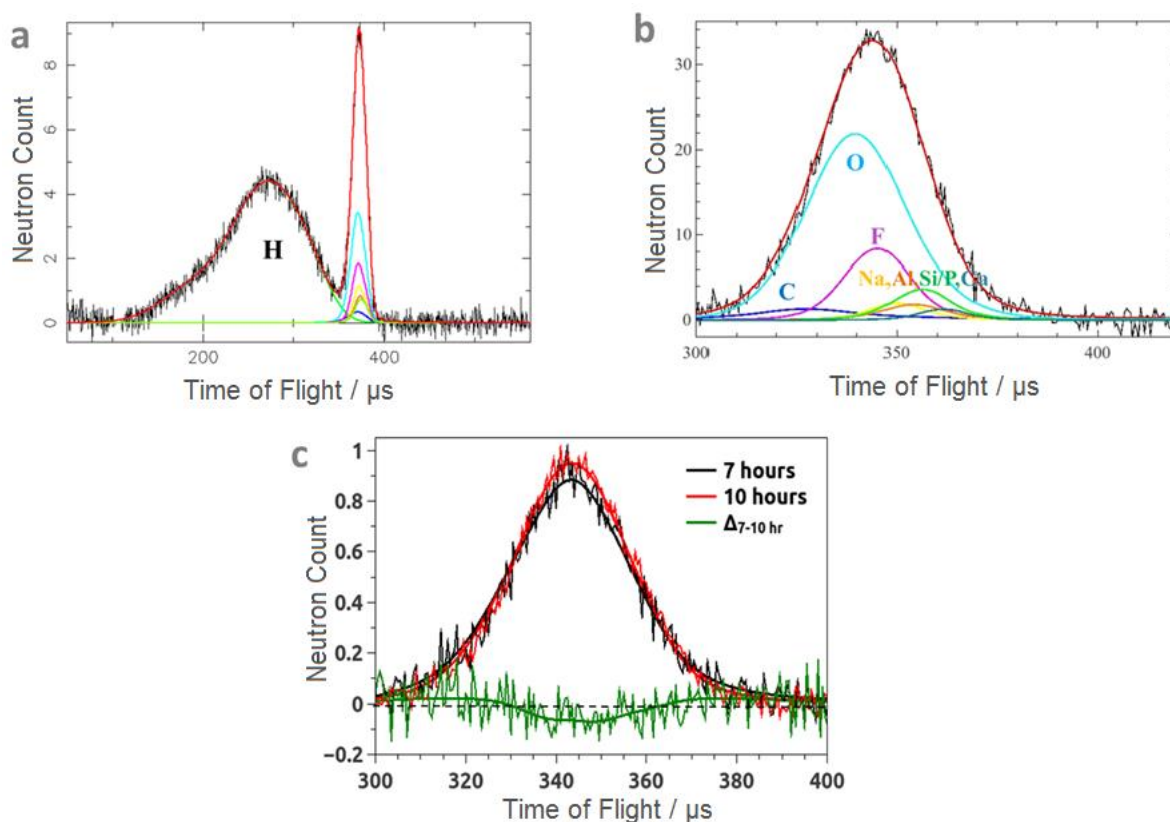
If you believe that this document breaches copyright please contact us providing details, and we will remove access to the work immediately and investigate your claim.

tel: +44 1970 62 2400

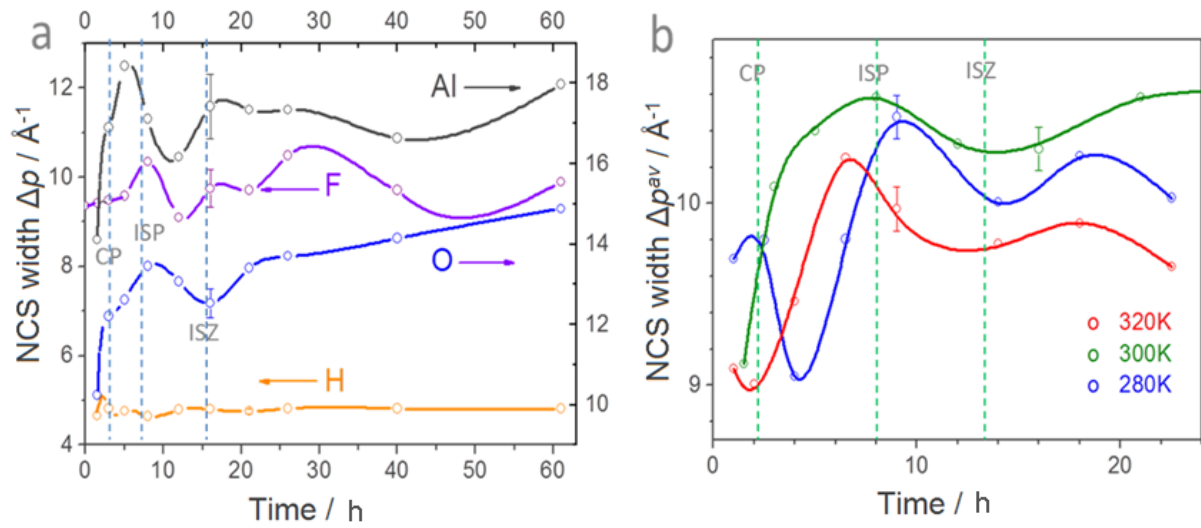
email: is@aber.ac.uk



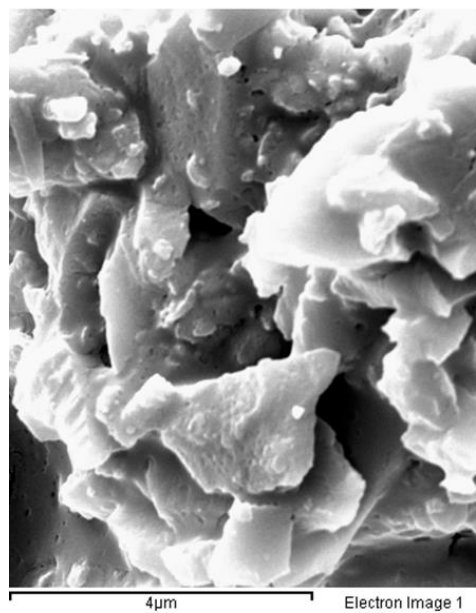
Supplementary Figure 1 | **a**: Isobaric heat capacity (C_p) (**a**) and mass change (**b**) as functions of temperature for the GIC sample after 62 hours setting, showing release of water and organic components.



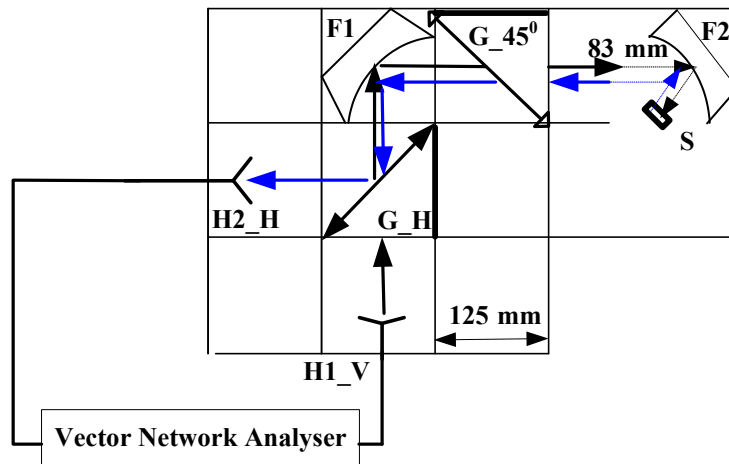
Supplementary Figure 2 | **a**, Example of forward scattering ToF data deconvoluted into elemental contributions by mass, each weighted by the stoichiometry. **b**, Corresponding backscattering peaks. **c**, NCS profiles (raw and fit data) of the total cement envelope at 7 and 10 hours, after initiation of setting; difference spectrum (raw and fitted data) is shown in green.



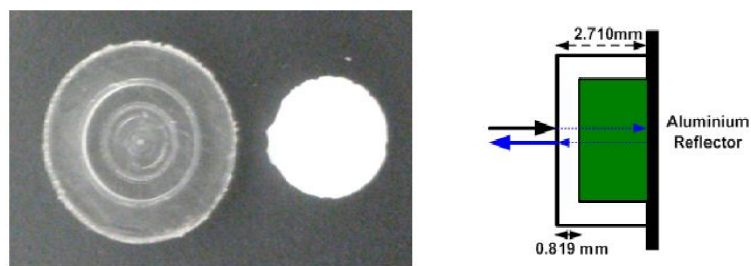
Supplementary Figure 3 | **a**, Elemental NCS peak widths Δp_i for H, O, F and Al. **b**, Average NCS peak widths $\sum_i c_i \Delta p_i$ for setting at 280 K, 300 K and 320 K, where c_i is the elemental atomic fraction. CP-coupling point, ISP-initial setting point, ISZ-intermediate stress zone; corresponding to early composite setting stages from Fig. 3.



Supplementary Figure 4 | SEM image of cement glass particles showing fractured surfaces.



Supplementary Figure 5 | Schematic diagram of the quasi-optical transmissometer. H1 and H2 denote a pair of corrugated feed-horns transceiver and the latter capital letter V and H present the linearly-vertical and horizontal polarised electric fields, respectively; F1, is an ellipsoidal reflector with focal length 250 mm and F2, a spherical mirror with focal length 83 mm; G_H presents a wire-grid with horizontal polarization and G_45⁰ stands for a wire-grid with 45⁰ polarization and S is the sample under test.



Supplementary Figure 6 | (left) Real TPX[®] cap and GIC; (right) the schematic plot of TPX[®] cap and the samples under the test are fully filled in the green area.